Design and simulation of structurally decoupled 4-DOF MEMS vibratory gyroscope

Ankush Jain* and Ram Gopal
MEMS and Microsensors Group
CSIR-Central Electronics Engineering Research Institute (CEERI)
Pilani, India
e-mail: *ankush@ceeri.ernet.in

***Abstract*—This paper presents design of a structurally decoupled 4-DOF MEMS vibratory gyroscope with increased robustness and gain. The proposed design utilizes dynamic amplification in 2-DOF drive mode oscillator and 2-DOF sense mode oscillator to achieve large gain. The device performance is verified through system level simulations in CoventorWare® ARCHITECT3D (SABER) platform, considering 10 µm thick nickel as structural layer. A wide operational bandwidth of 704 Hz is achieved. Moreover to verify the device performance under the application of angular velocity, a rate table simulation is carried out which resulted in sense mass displacement of 136.2 nm corresponding to the rotation induced Coriolis force at actuation voltage of 20 V_{ac} and 40 V_{dc} with angular rotation of 35 rad/s.**

Keywords-4-DOF vibratory gyroscope; simulation; UV-LIGA

I. INTRODUCTION

In two degees-of-freedom (2-DOF) MEMS vibratory gyroscope, a single proof mass is driven into resonance by an external sinusoidal force. If both the drive and sense mode have the same resonant frequencies, the rotation induced Coriolis force excites the system into resonance in the secondary sense direction and the sensor output increases at the cost of reduced mechanical bandwidth [1]. However, achieving resonance in both drive and sense modes becomes extremely difficult in the presence of environmental variations and fabrication imperfections, induced due to tolerance capabilities of the photolithography processes and fabrication techniques. Thus, in 2-DOF gyroscopes, an active feedback control system with direction electronics becomes inevitable to minimize the effects of unavoidable fabrication flaws and environmental variations. This problem can be solved by utilizing the frequency mismatching techniques in designing the operational modes of the device [2], but these results in decreased gain. Recently new design approaches have been implemented utilizing multi-DOF with increased robustness to fabrication imperfections and environmental variations and high gain [3]-[5].

The proposed design of 4-DOF vibratory gyroscope provides inherent robustness by achieving large operational bandwidth. It utilizes dynamic amplification to achieve large oscillation amplitudes without resonance, while mechanically decoupling the drive direction oscillations from the sense direction oscillations. The device will be fabricated using UV-LIGA technique having 10 µm thick Nickel as structural layer. The details of UV-LIGA technique can be found in [6].

The paper is organized as follow. Section II explains the operating principle of 4-DOF vibratory gyroscope along with the analytical values of optimized design. Complete 3-D behavioral model of the device is successfully developed and frequency analysis, dynamic amplification analysis and rate table characterization is carried out in Section III.

II. OPERATING PRINCIPLE OF 4-DOF VIBRATORY GYROSCOPE

The proposed design of 4-DOF vibratory gyroscope utilizes dynamical amplification in the 2-DOF drive mode oscillators and structurally decoupled 2-DOF sense mode oscillators in order to achieve large oscillation amplitudes without resonance. The frequency responses of the 2-DOF drive direction oscillator and the 2-DOF sense direction oscillator have two resonant peaks and a flat region between them. The device is nominally operated in the flat regions of the drive and sense direction oscillators, where the response amplitudes of the oscillators are less sensitive to parameter variations. The overall 4-DOF dynamical system, namely 2-DOF in drive and 2-DOF in sense directions, is composed of three interconnected proof masses. The conceptual schematic of 4-DOF vibratory gyroscope is shown in Fig. 1.

The first mass m_1 (active mass of 2-DOF drive mode oscillator) which is the only mass excited in the drive direction, is constrained in the sense direction, and is free to oscillate only in the drive direction. The second mass m_2 and third mass m_3 are constrained with respect to each other in the drive direction, thus oscillating as one combined mass, $(m_2 + m_3)$ (passive mass of 2-DOF drive mode oscillator) in the drive direction. However, m_2 (active mass of 2-DOF sense mode oscillator) and m_3 (passive mass of 2-DOF sense mode oscillator) are free to oscillate independently in the sense direction, forming the 2-DOF sense mode oscillator. The first mass m_1 and the combination of the second and third masses $(m_2 + m_3)$ form the 2-DOF drive mode oscillator.

In order to minimize quadrature error and bias due to dynamical coupling between the drive and sense modes, the drive and sense direction oscillators are mechanically decoupled. The driven mass m_1 oscillates only in the drive direction, and possible anisoelasticities due to fabrication imperfections are suppressed by the suspension fixed in the sense direction. The second mass m_2 oscillates in both drive and sense directions, and generates the rotation induced

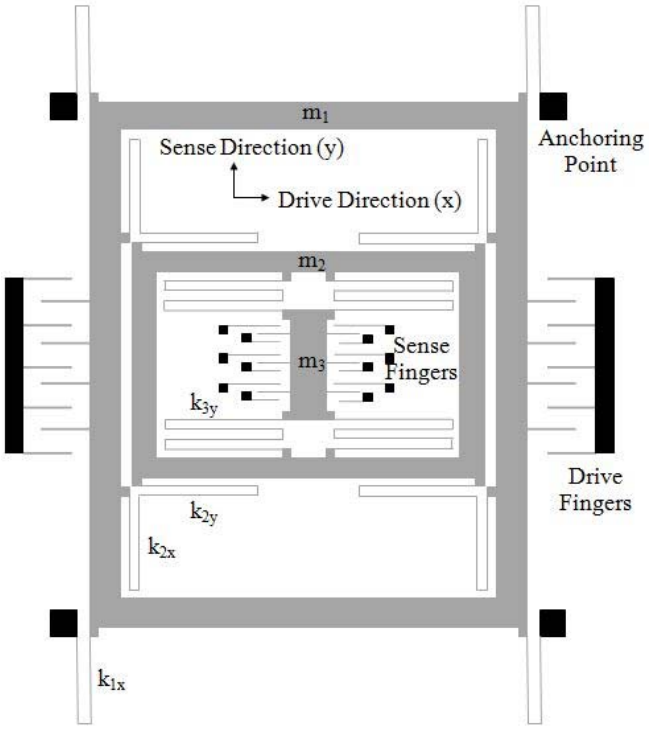

Figure 1. Conceptual schematic of 4-DOF vibratory gyroscope

Coriolis force that excites the 2-DOF sense mode oscillator. The sense direction response of the third mass m_3 which comprises the vibration absorber of the 2-DOF sense mode oscillator is detected for measuring the input angular rate. Since the springs that couple the sense element m_3 to m_2 deform only for relative sense direction oscillations, mechanical coupling of the drive mode oscillations into the sense mode of m_3 is minimized, significantly enhancing gyroscopic performance.

The objectives of design optimization are: to achieve large operational bandwidth both in drive and sense directions, to have sense direction capacitance change of the order of *f*F and the overall design should be such that it can be fabricated using UV-LIGA fabrication technique having 10 μm thick Nickel as structural layer. Table I shows the summary of the design parameters for the optimized design.

TABLE I. SUMMARY OF THE OPTIMIZED DESIGN PARAMETERS

Parameters	Analytical values
m_1	5.31×10^{-7} kg
m_2	1.8×10^{-7} kg
m_3	2.11×10^{-8} kg
k_{1x}	83.85 N/m
k_{2x}	38.37 N/m
k_{2y}	28.42 N/m
k_{3y}	3.33 N/m
$\omega_{1x}=\sqrt{k_{1x}/m_1}$	2 kHz
$\omega_{2x}=\sqrt{k_{2x}/(m_2+m_3)}$	2 kHz
$\omega_{2y}=\sqrt{k_{2y}/m_2}$	2 kHz
$\omega_{3y}=\sqrt{k_{3y}/m_3}$	2 kHz
Resonance frequencies (Drive)	1.43 kHz, 2.79 kHz
Resonance frequencies (Sense)	1.68 kHz, 2.37 kHz

A. Proposed gyroscope dynamics

The lumped model of proposed design is shown in Fig. 2. The first mass m_1 and the combination of second and third masses (m_2+m_3) form 2-DOF drive direction oscillator, where m_1 is the driven mass. The second mass m_2 and the third mass m_3 form 2-DOF sense direction oscillator. The equations of motion (along the x-axis and y-axis) of the three mass system subjected to an angular rate Ω about the axis normal to the plane of motion (z-axis) can be expressed in the inertial frame as

$$m_1\ddot{x}_1 + c_{1x}\dot{x}_1 + k_{1x}x_1 = k_{2x}(x_2 - x_1) + F_d \quad (1)$$

$$(m_2+m_3)\ddot{x}_2 + (c_{2x}+c_{3x})\dot{x}_2 + k_{2x}(x_2 - x_1) = 0 \quad (2)$$

$$m_2\ddot{y}_2 + c_{2y}\dot{y}_2 + k_{2y}y_2 = k_{3y}(y_3 - y_2) - 2m_2\Omega\dot{x}_2 \quad (3)$$

$$m_3\ddot{y}_3 + c_{3y}\dot{y}_3 + k_{3y}(y_3 - y_2) = -2m_3\Omega\dot{x}_3 \quad (4)$$

where, m_1, m_2, m_3 are masses; $c_{1x}, c_{2x}, c_{2y}, c_{3y}$ are damping coefficients; $k_{1x}, k_{2x}, k_{2y}, k_{3y}$ are spring constants; $F_d = f_o sin\omega_d t$ is electrostatic driving force having ω_d as driving frequency.

The first mass m_1 is fixed in the sense direction i.e. $y_1(t) = 0$. The second mass m_2 and the third mass m_3 move together in the drive direction, i.e. $x_2(t) = x_3(t)$. While deriving equations of motion, it is assumed that Coriolis terms in drive direction and centripetal accelerations are zero. Angular rate Ω is considered to be constant.

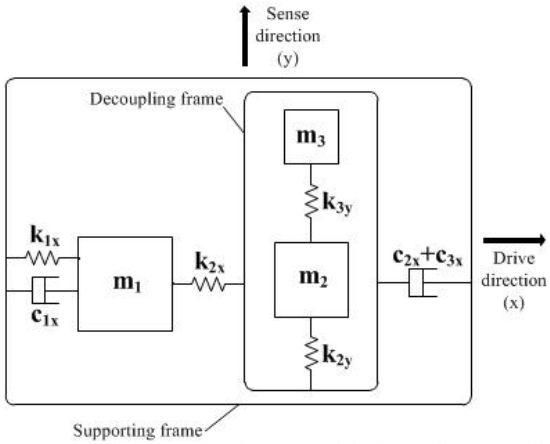

Figure 2. Lumped mass-spring-damper model of overall 4-DOF vibratory gyroscope

III. SIMULATIONS

CoventorWare® ARCHITECT3D (SABER) suite (CoventorWare 2010) is used to verify the analytically optimized design by system level simulation of the gyroscope. The symbols representing the individual components are connected and parameterized in the schematic to represent a three dimensional MEMS device. The main components used are rigid plate, beam and comb-drive. Fig. 3(a) shows the complete schematic model of the 4-DOF vibratory gyroscope. Fig. 3(b) shows the 3-D model of gyroscope generated by SABER based on the schematic.

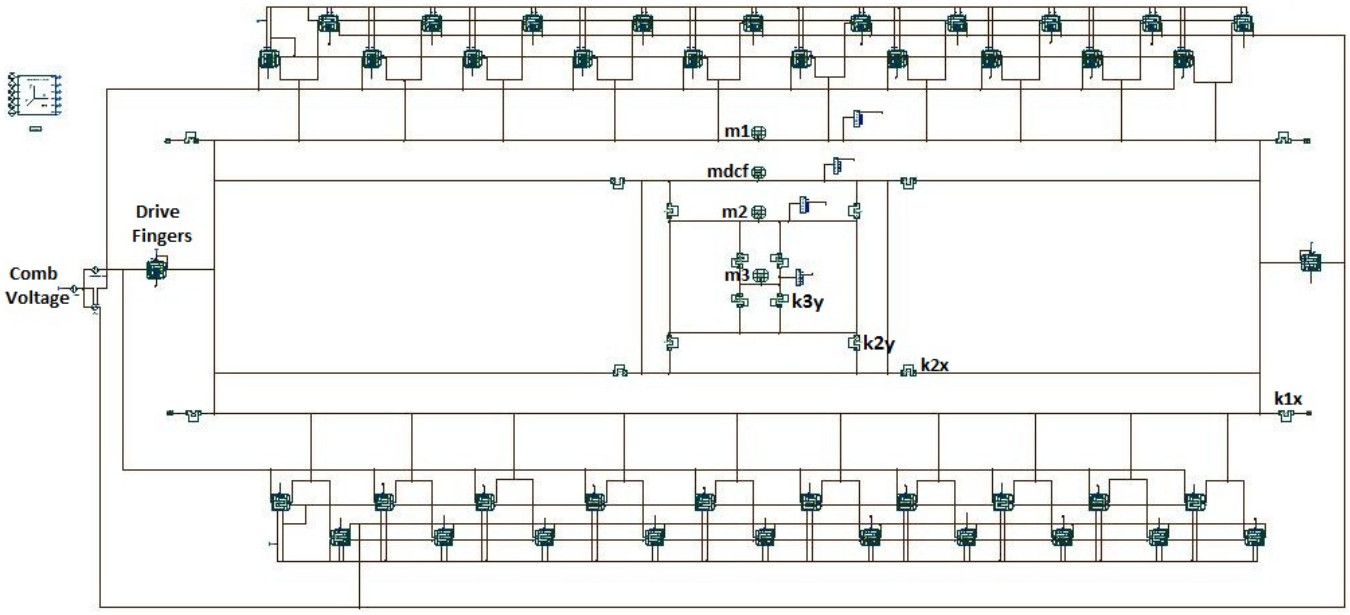

(a)

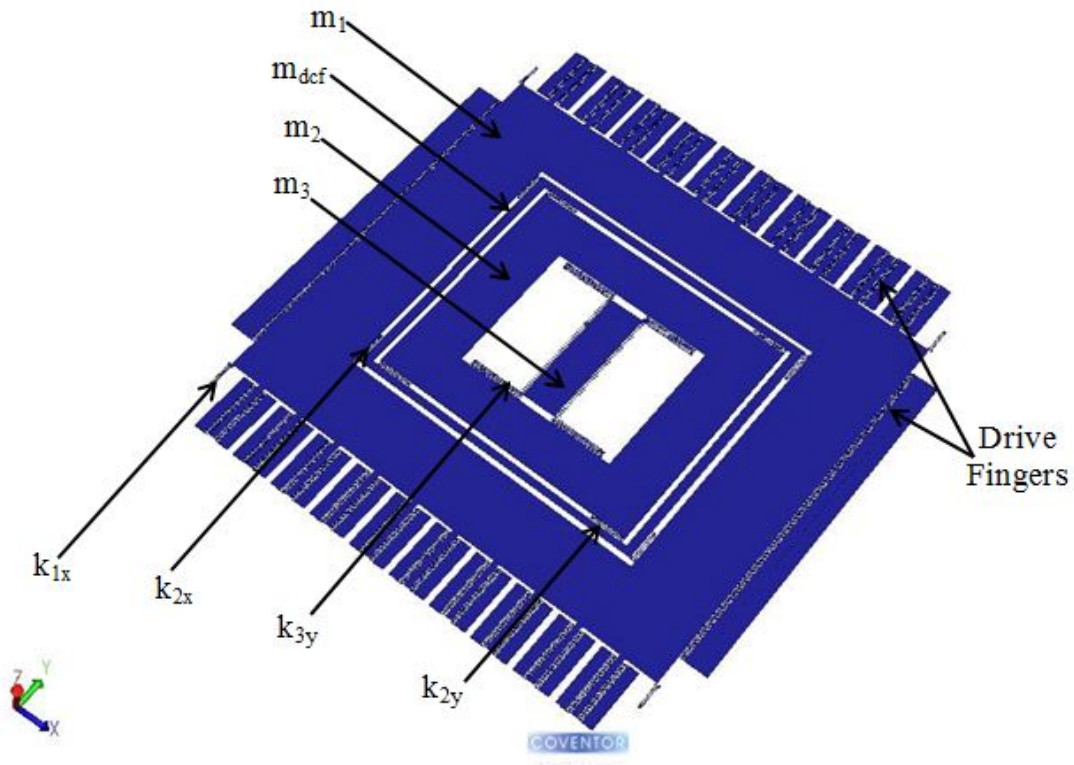

(b)

Figure 3. (a) Schematic model of 4-DOF vibratory gyroscope (b) 3-D model of gyroscope generated by SABER

A. Frequency and dynamic amplification analysis

When a constant amplitude sinusoidal force $F_d = f_0 sin(\omega_d t)$ is applied on the active mass m_1, the steady state response of the 2-DOF drive mode oscillator is

$$X_1(j\omega) = \frac{\frac{f_0}{k_{1x}}\left\{1-\left(\frac{\omega}{\omega_{2x}}\right)^2 + j\frac{c_{2x}}{k_{2x}}\omega\right\}}{\left\{1-\left(\frac{\omega}{\omega_{1x}}\right)^2 + \frac{k_{2x}}{k_{1x}} + j\frac{c_{1x}}{k_{1x}}\omega\right\}\left\{1-\left(\frac{\omega}{\omega_{2x}}\right)^2 + j\frac{c_{2x}}{k_{2x}}\omega\right\} - \frac{k_{2x}}{k_{1x}}} \quad (5)$$

$$X_2(j\omega) = \frac{\frac{f_0}{k_{1x}}}{\left\{1-\left(\frac{\omega}{\omega_{1x}}\right)^2 + \frac{k_{2x}}{k_{1x}} + j\frac{c_{1x}}{k_{1x}}\omega\right\}\left\{1-\left(\frac{\omega}{\omega_{2x}}\right)^2 + j\frac{c_{2x}}{k_{2x}}\omega\right\} - \frac{k_{2x}}{k_{1x}}} \quad (6)$$

where $\omega_{1x} = \sqrt{k_{1x}/m_1}$ and $\omega_{2x} = \sqrt{k_{2x}/(m_2+m_3)}$ are the resonant frequencies of the isolated active and passive mass-spring-damper system respectively in drive direction. When the driving frequency, $\omega_d = \omega_{2x}$ the passive mass moves to exactly cancel out the applied input force F_d on the active mass, and maximum dynamic amplification is achieved.

Sense mode oscillator is driven by the rotation induced Coriolis force $F_{c2} = -2m_2\,\Omega\dot{x}_2$ and $F_{c3} = -2m_3\,\Omega\dot{x}_2$ generated by m_2 and m_3 respectively. The steady state response is given by

$$Y_2(j\omega) = \frac{-j2\Omega\omega X_2(j\omega)\left[m_2\left\{1-\left(\frac{\omega}{\omega_{3y}}\right)^2 + j\frac{c_{3y}}{k_{3y}}\omega\right\} + m_3\right]}{k_{2y}\left[\left\{1-\left(\frac{\omega}{\omega_{2y}}\right)^2 + \frac{k_{3y}}{k_{2y}} + j\frac{c_{2y}}{k_{2y}}\omega\right\}\left\{1-\left(\frac{\omega}{\omega_{3y}}\right)^2 + j\frac{c_{3y}}{k_{3y}}\omega\right\} - \frac{k_{3y}}{k_{2y}}\right]} \quad (7)$$

$$Y_3(j\omega) = \frac{-j2\Omega\omega X_2(j\omega)\left[m_3\left\{1-\left(\frac{\omega}{\omega_{2y}}\right)^2 + \frac{k_{3y}}{k_{2y}} + j\frac{c_{2y}}{k_{2y}}\omega\right\} + m_2\frac{k_{3y}}{k_{2y}}\right]}{k_{3y}\left[\left\{1-\left(\frac{\omega}{\omega_{2y}}\right)^2 + \frac{k_{3y}}{k_{2y}} + j\frac{c_{2y}}{k_{2y}}\omega\right\}\left\{1-\left(\frac{\omega}{\omega_{3y}}\right)^2 + j\frac{c_{3y}}{k_{3y}}\omega\right\} - \frac{k_{3y}}{k_{2y}}\right]} \quad (8)$$

where $\omega_{2y} = \sqrt{k_{2y}/m_2}$ and $\omega_{3y} = \sqrt{k_{3y}/m_3}$ are the resonant frequencies of the isolated active and passive mass-spring-damper system respectively in sense direction. When the frequency of the sinusoidal Coriolis force is matched with the resonant frequency of the isolated passive mass-spring system, the passive mass achieves maximum dynamic amplification.

To verify the device's frequency characteristics, frequency analysis is carried out in CoventorWare® ARCHITECT3D (SABER) platform by varying the frequency from 1 Hz to 4 kHz. The results are shown in Fig. 4. Two resonance frequencies for the 2-DOF drive mode oscillator are located at 1.412 kHz and 2.753 kHz, which matches well to analytically calculated values of 1.43 kHz and 2.79 kHz as shown in Table I. Two resonance frequencies for the 2-DOF sense mode oscillator are located at 1.638 kHz and 2.342 kHz, which matches well to analytically calculated values of 1.68 kHz and 2.37 kHz as shown in Table I.

In the case of dual mass oscillator it is observed [7] that at first resonant frequency, active and passive masses are in phase and maximum dynamic amplification is achieved while at second resonant frequency active and passive masses are out of phase and thus dynamic amplification is negligible. To verify the dynamical amplification concept, frequency analysis is carried out at 40 V_{dc} and 20 V_{ac}. In our design, there are two dual mass oscillators, one in drive direction and the other in sense direction. Fig. 4(a) shows the amplitude and phase response of drive direction dual mass oscillator. It is observed that in the drive mode at first resonance frequency i.e. 1.412 kHz active and passive masses, with response amplitudes of -72.61 dB (234.1 μm) and -66.36 dB (480.6 μm) respectively, are in phase and dynamical amplification of 2.05 times is achieved while at second resonance frequency both the masses are 179.79° out of phase and dynamic amplification is not pronounced. However, in the flat operating region between the two resonance peaks specifically at 2 kHz, response amplitudes of both active and passive masses are -140.2 dB (97.27 nm) and -111.1 dB (2.791 μm) respectively, with a dynamic amplification of 28.69 times. Fig. 4(b) shows the amplitude and phase response of sense direction dual mass oscillator. It is observed that in the sense mode at first resonance frequency i.e. 1.638 kHz active and passive masses, with response amplitudes of -123.2 dB (0.69 μm) and -112.3 dB (2.42 μm) respectively, are in phase and dynamical amplification of 3.51 times is achieved while at second resonance frequency both the masses are 173.11° out of phase and negligible dynamic amplification is pronounced. However, in the flat operating region between the two resonance peaks specifically at 2 kHz, response amplitudes of both active and passive masses are -159.3 dB (10.81 nm) and -137.1 dB (140.2 nm) respectively, with a dynamic amplification of 12.97 times.

This frequency analysis verifies the working of the proposed design as dual mass oscillator and thus achieving dynamic amplification for increased sensitivity.

B. Transient analysis and rate table simulation

Transient analysis simulates the response of a device to any time-varying input and is most often used to simulate responses similar to what one might measure on a fabricated device [8]. To verify the response time as well as the detection amplitude of the gyroscope, transient analysis is also carried out in CoventorWare® ARCHITECT3D (SABER) platform at 40 V_{dc} and 20 V_{ac} with constant angular rate of 35 rad/s. Driving frequency is kept as 2 kHz. The result is shown in Fig. 5. The steady state amplitude of sense mass m_3 is 136.2 nm. Capacitance change of 4.29 fF is

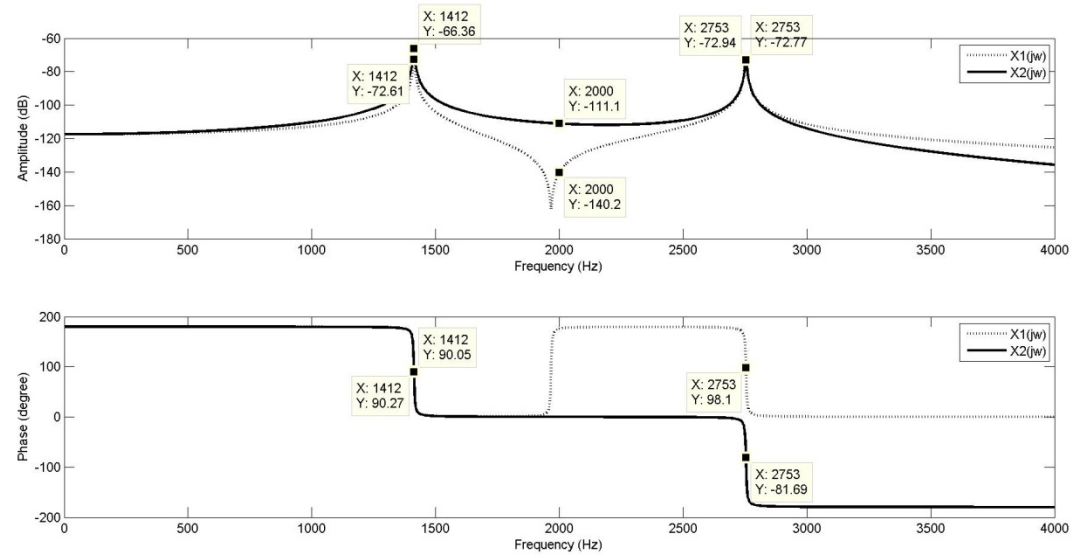

(a)

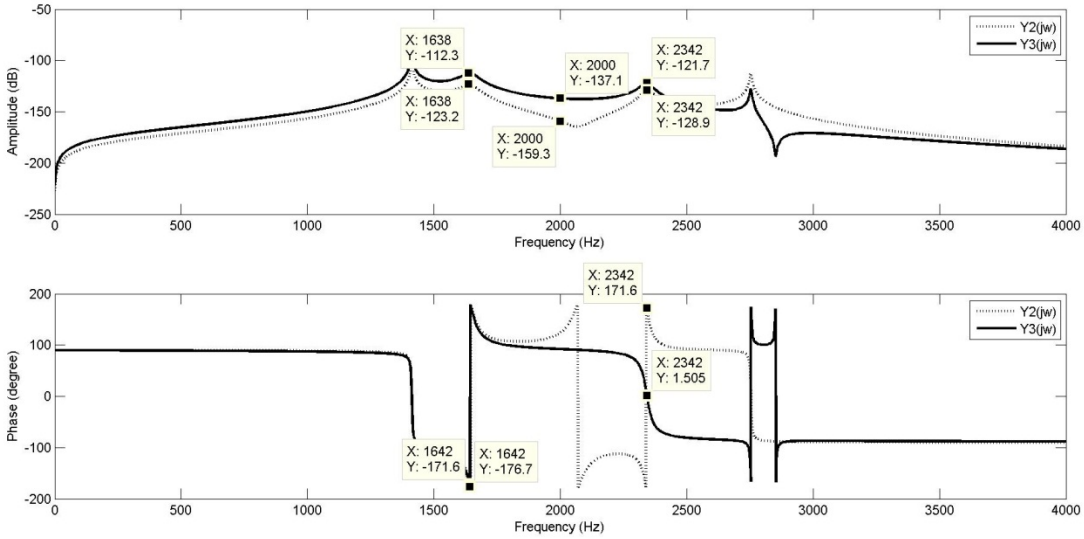

(b)

Figure 4. (a) Frequency response of drive direction oscillator (b) Frequency response of sense direction oscillator

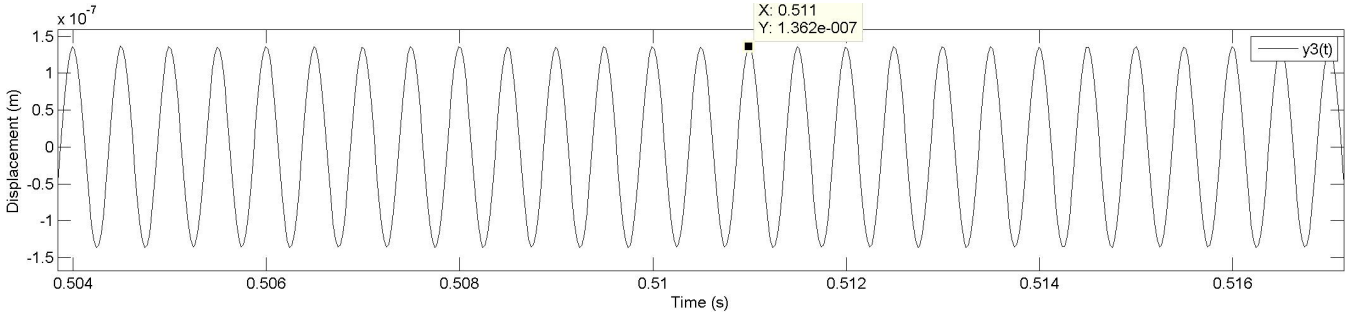

Figure 5. Steady state transient response of sense mass m_3

achieved in sense combs using the differential capacitance scheme.

IV. CONCLUSION

A MEMS vibratory gyroscope design concept with 2-DOF drive mode oscillator and structurally decoupled 2-DOF sense mode oscillator is presented. The prototype with an overall chip size of 5mm×5mm is designed to be fabricated using UV-LIGA technique having 10 μm thick Nickel as structural layer. A system level simulation of the device is carried out. A wide operational bandwidth of 704 Hz is achieved. To analyse the device performance under the application of angular velocity, a rate table simulation is also carried out. Capacitance change of 4.29 fF is achieved in sense combs using differential capacitance configuration.

ACKNOWLEDGEMENT

The authors would like to thank Dr. Chandra Shekhar, Director, CEERI for financial and motivational support and IC Design Group, CEERI for providing access to MEMS CAD tool Coventorware®.

REFERENCES

[1] C. Acar, A.M. Shkel, L. Costlow, and A.M. Madni, "Inherently robust micromachined gyroscopes with 2-DOF sense-mode oscillator," IEEE Sensors Conference, Irvine, California, pp. 664-667, Oct. 30 2005-Nov. 3 2005.

[2] A.R. Schofield, A.A. Trusov, and A.M. Shkel, "Effects of operational frequency scaling in multi-degree of freedom MEMS gyroscopes," IEEE Sensors Journal, vol.8, no.10, pp.1672-1680, Oct. 2008.

[3] Seung-Hoon Jeon, June-Young Lee, Hyoung-Kyoon Jung, Hyun-Kee Chang, and Yong-Kweon Kim, "Two-mass system with wide bandwidth for SiOG (silicon on glass) vibratory gyroscopes," The 13th International Conference on Solid-State Sensors, Actuators and Microsystems, Seoul, Korea, vol.1, pp. 539- 542, 5-9 June 2005.

[4] C. Acar and A.M. Shkel, "Inherently robust micromachined gyroscopes with 2-DOF sense-mode oscillator," Journal of Microelectromechanical Systems, vol.15, no.2, pp. 380- 387, April 2006.

[5] C. Acar and A.M. Shkel, "Non-resonant micromachined gyroscopes with structural mode-decoupling," IEEE Sensors Journal, vol. 3, no. 4, pp. 497-506, Aug. 2003.

[6] Wenmin Qu, C. Wenzel, A. Jahn, and D. Zeidler, "UV-LIGA: a promising and low-cost variant for microsystem technology," Proceedings of conference on Optoelectronic and Microelectronic Materials Devices, pp.380-383, 1999.

[7] C.W. Dyck, J. Allen, and R. Hueber, "Parallel plate electrostatic dual mass oscillator", Proceedings of SPIE, SOE, CA, 1999.

[8] CoventorWare ARCHITECT, Version 2008, Reference: MEMS and microsystems system- level design.